2020 IEEE/RSJ International Conference on Intelligent Robots and Systems (IROS)
October 25-29, 2020, Las Vegas, NV, USA (Virtual)

A Model-Free Solution for Stable Balancing and Locomotion of Floating-base Legged Systems

Emmanouil Spyrakos-Papastavridis[1,2], Jian S. Dai[1]

Abstract—**This paper presents novel control techniques for passivation and stabilisation of floating-base systems with contacts, whose dynamical models comprise both joint-space, and Cartesian floating-base coordinates. The aforementioned results are achieved using both minimally model-based, and completely model-free controllers that employ power-shaping signals. Model-free control is permitted through usage of a decoupled dynamical model, procured via coordinate transformation operations. It is demonstrated that even though passive closed-loop systems are attainable without utilisation of exteroceptive feedback, global stabilisation of a floating-base robot necessitates direct usage of either measured or estimated external forces. The presented asymptotical stabilisation results pertain to both the set-point regulation, and trajectory-tracking cases, thereby ensuring suitability for static balancing, and dynamical locomotion tasks. To ensure practicability and production of feasible input signals, a variable impedance control, power-shaping term is appended to the original design, wherein it circumstantially serves as either a power-dissipating, or power-injecting element. This enhancement provably preserves closed-loop stability, by appositely shaping the system's power. Experiments involving a metamorphic, quadrupedal walking robot, corroborate the theoretical analysis, as they attest to the system's ability to stably execute locomotory tasks using a single, unified, model-free control scheme.**

I. Introduction

THE vast majority of biological legged machines that exist in nature, exhibit remarkable performance in terms of dexterity, balancing, speed, agility, and interaction. In spite of this phenomenon, one rarely witnesses their artificial counterparts display similar abilities, despite the numerous scientific exertions that have aimed at the development of biomimetic robots. One of the main challenges that currently impedes widespread use of these machines, is the efficient control of their inherent under-actuated Degrees-of-Freedom (DoFs), which is also deemed an open problem in the field [1]. However, under-actuation may have distinct manifestations, depending on the robotic system under consideration. For example, there exists the purely structural form of under-actuation, relating to a robot's inherent joint or link properties; this category encompasses soft link [2] and soft joint [3] robots. The latter field has received considerable attention spanning nearly three decades, with one of the early works [4] demonstrating that a Proportional-Derivative (PD) plus gravity compensation controller, suffices for global stabilisation around a set point. The more challenging problem of flexible-joint robot tracking control, has been addressed in a limited number of treatises [5]-[8] that propound manifold model-based controller designs.

Soft link robots, such as continuum devices [2][9], are occasionally considered hyper-redundant, which further increases modelling and control complexity, as compared to flexible-joint robots. Analytical methods for provable convergence of these robots are unavailable, when excluding utilisation of reduced-order models [10].

Legged robots belong to an aberrant sub-category of under-actuated devices, as they can alternate between fully-actuated, over-actuated, and under-actuated modes, in almost immediate succession. Full actuation is typically observed when a legged robot (such as a biped) assumes a single support stance on a flat surface (full contact), over-actuation occurs during the double support phase, and under-actuation arises when full contact with the floor cannot be maintained during a support phase. The previously described erratic dynamics, has traditionally forced roboticists to resort to overly simplified representations, such as the Linear Inverted Pendulum Model (LIPM) [11], for the purpose of devising balancing and locomotion control algorithms. However, mechanical devices with the ability to freely locomote in space, can be mathematically described with a high degree of accuracy, using the floating-base models that were initially introduced in [12]-[14]. Since the aforesaid methods are predominantly intended for use on space robots, the modelling and handling of external contacts is not deemed to be of paramount importance, and is consequently disregarded. To this end, a method of augmenting a free-floating humanoid robot model, via indirect incorporation of contact/task forces, is delineated in [15]. An extension to the latter is provided through [16], wherein the overall dynamical model offers a representation comprising the floating-base coordinates, joint coordinates, and contact forces. Utilisation of the previously described model has enabled the development of manifold model-based control algorithms for legged robots. [17] outlines a methodology for effective computation of an inverse dynamics controller that is directly implementable on floating-base systems with contact constraints. [18] proposes a modified form of the original floating-base dynamical model, for the purpose of achieving a decoupling between the floating-base and joint-space dynamics, thereby leading to immense simplification of the mathematical model. A contact-based, gravity compensation torque controller is subsequently implemented, to compensate for the under-actuated (non-collocated) gravitational terms. [19] presents an analytically sound solution to the inverse dynamics control of floating-base systems, by means of orthogonal decomposition, which obviates the need for contact force feedback. [20] delineates an inverse dynamics controller that achieves optimal contact force distribution, via exploitation of toque redundancy. [21]

[1]E. Spyrakos-Papastavridis and J. S. Dai are with the Department of Engineering, King's College London, Strand, London, WC2R 2LS, United Kingdom, {emmanouil.spyrakos, jian.dai} at kcl.ac.uk.
[2]E. Spyrakos-Papastavridis is with the Dyson School of Design Engineering, Imperial College London, South Kensington, London, SW7 2AZ, United Kingdom, {e.spyrakos-papastavridis} at imperial.ac.uk.

demonstrates that a hierarchical cascade of quadratic programs containing dynamical models, equality/inequality constraints, and contacts, could enable generation of complex humanoid robot motions. [22] describes the adaptation and implementation of a hierarchical inverse dynamics controller to a physical humanoid robot, which enables performance of balancing tasks. Moreover, [23] delineates a control scheme that amalgamates a passivity-based controller, with a task hierarchy algorithm, leading to a unified balancing framework for torque-controlled bipeds. Contrariwise, [24] suggests that usage of simple LQR controllers, could offer performance levels that are almost equatable with those yielded by involute, optimisation-based schemes. Employment of LQR techniques for the design of highly under-actuated, passively compliant humanoid balancing controllers, is reported in [25][26].

Even though several legged robot controllers [22][27] are numerically stable, eliciting comprehensive stability analyses for these systems, is a complex task. Scrutinising the relevant literature reveals the existence of a limited number of stability analyses for floating-base legged robots [23][28][18]. One such example is the regulation stability analysis presented in [23] that relies upon satisfaction of imposed contact-force constraints. Moreover, the regulation stability study proposed in [28] requires linearization of the closed-loop dynamics, while [18] provides a passivity analysis that avoids differentiation of the proposed storage function. Contrarily, this article proposes minimally model-based, and model-free controllers that demonstrably induce passivity and global tracking stability into floating-base systems with contacts, which to the best of the authors' knowledge, has not hitherto been reported elsewhere. The proposed design idea employs a solution to under-actuation that is analogous to those in [29][30], and could therefore be perceived as a legged-robot extension to these works.

The rest of the paper is structured as follows; section II presents minimally model-based control schemes for floating-base legged robots with contacts, section III introduces model-free controllers for legged machines, and section IV describes the experimental results. Finally, section V offers the conclusion.

II. Minimally Model-Based Control of Floating-Base Legged Systems with Contacts

A. Floating-base Dynamics with Contacts

The dynamics of an n-DoF floating-base robot with contacts (Fig. 1), may be represented as follows [16][17]:

$$\mathbf{M_{fb}}\ddot{\boldsymbol{q}}_{\boldsymbol{fb}} + \mathbf{C_{fb}}\dot{\boldsymbol{q}}_{\boldsymbol{fb}} + \boldsymbol{G}_{\boldsymbol{fb}} = \begin{bmatrix}\mathbf{0}\\ \boldsymbol{\tau_m}\end{bmatrix} + \begin{bmatrix}\mathbf{J}_{\mathbf{c_b}}^{\mathrm{T}}\boldsymbol{f_p}\\ \mathbf{J}_{\mathbf{c_j}}^{\mathrm{T}}\boldsymbol{f_p}\end{bmatrix}, \qquad (1)$$

where the inertia matrix $\mathbf{M_{fb}} \in \mathbb{R}^{(n+6)\times(n+6)} = \begin{bmatrix}\mathbf{M_{bb}} & \mathbf{M_{bj}}\\ \mathbf{M_{jb}} & \mathbf{M_{jj}}\end{bmatrix}$, comprises the $\mathbf{M_{bb}} \in \mathbb{R}^{6\times6}$, $\mathbf{M_{bj}} \in \mathbb{R}^{6\times n}$, and $\mathbf{M_{jj}} \in \mathbb{R}^{n\times n}$ terms, while $\boldsymbol{G}_{\boldsymbol{fb}} \in \mathbb{R}^{n+6} = \begin{bmatrix}\mathbf{M_{bb}}g\boldsymbol{S_s}\\ \mathbf{M_{jb}}g\boldsymbol{S_s}\end{bmatrix}$, with $\boldsymbol{S_s} = [0_{1\times2}\ \ 1\ \ 0_{1\times3}]^T$. $\mathbf{J_{c_b}} \in \mathbb{R}^{6\times6}$ and $\mathbf{J_{c_j}} \in \mathbb{R}^{6\times n}$ signify contact Jacobians. The vector $\boldsymbol{q_{fb}} = \begin{bmatrix}\boldsymbol{q_b}^T & \boldsymbol{q_j}^T\end{bmatrix}^T$, contains $\boldsymbol{q_j} \in \mathbb{R}^n$ and $\boldsymbol{q_b} \in \mathbb{R}^6$, which denote the joint-space and floating-base coordinates, respectively, $\mathbf{C_{fb}} \in \mathbb{R}^{(n+6)\times(n+6)}$ represents the matrix of Coriolis and centrifugal terms, g signifies the acceleration of gravity, $\boldsymbol{f_p} \in \mathbb{R}^6$ symbolises the constraint force, and $\boldsymbol{\tau_m} \in \mathbb{R}^n$ denotes the input signal vector.

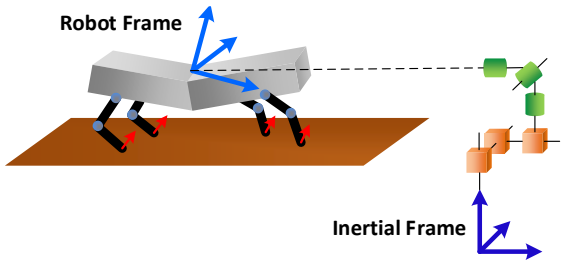

Figure 1. Schematic of a metamorphic quadrupedal floating-base robot.

For the multi-contact case, $\boldsymbol{f_p} \in \mathbb{R}^{6\delta}$, $\mathbf{J_{c_b}} \in \mathbb{R}^{6\delta\times6}$, and $\mathbf{J_{c_j}} \in \mathbb{R}^{6\delta\times n}$, with δ denoting the number of contacts.

B. Regulation Control of Floating-base Systems

Although regulation controllers are, from a theoretical standpoint, unsuitable for locomotion tasks, they are useful for static balancing, where exploitation of the inherent dynamics is desirable. The following regulator is proposed:

$$\boldsymbol{\tau_m} = \mathbf{K_P}\boldsymbol{q}_{\boldsymbol{j_E}} - \mathbf{K_D}\dot{\boldsymbol{q}}_{\boldsymbol{j}} + \mathbf{M_{jb}}g\boldsymbol{S_s} + \boldsymbol{\nu_P}\left(\dot{\boldsymbol{q}}_{\boldsymbol{b}}^T\mathbf{M_{bb}}g\boldsymbol{S_s}\right), \qquad (2)$$

with $\boldsymbol{\nu_P} \in \mathbb{R}^n = \dot{\mathbf{Q}}_{\mathbf{S}} \cdot [1 \dots 1_n]^T \cdot rank\left(\dot{\mathbf{Q}}_{\mathbf{S}}\right)^+$, $\dot{\mathbf{Q}}_{\mathbf{S}} \in \mathbb{R}^{n\times n} = diag\left(\dot{\boldsymbol{q}}_{\boldsymbol{j}}\right)^+$, $\boldsymbol{q}_{\boldsymbol{j_E}} = \boldsymbol{q}_{\boldsymbol{j_d}} - \boldsymbol{q}_{\boldsymbol{j}}$, while $\mathbf{K_P}$, $\mathbf{K_D} \in \mathbb{R}^{n\times n}$ denote diagonal, positive definite, proportional and derivative gain matrices, respectively. The scalar term $rank\left(\dot{\mathbf{Q}}_{\mathbf{S}}\right)^+ > 0$, when $\left\|\dot{\mathbf{Q}}_{\mathbf{S}}\right\| \neq \mathbf{0}$, and is zero otherwise. Terms multiplied by $\boldsymbol{\nu_P}$, collectively comprise the Power-Shaping Signal (PSS).

Theorem 1: Implementing controller (2) onto the system described by (1), yields a passive system.

Proof 1: One may select the following storage function:

$$Q = \tfrac{1}{2}\dot{\boldsymbol{q}}_{\boldsymbol{fb}}^T\mathbf{M_{fb}}\dot{\boldsymbol{q}}_{\boldsymbol{fb}} + \tfrac{1}{2}\boldsymbol{q}_{\boldsymbol{j_{EI}}}^T\mathbf{K_P}\boldsymbol{q}_{\boldsymbol{j_{EI}}}, \qquad (3)$$

where $\boldsymbol{q}_{\boldsymbol{j_{EI}}} = \boldsymbol{q}_{\boldsymbol{j}} - \boldsymbol{q}_{\boldsymbol{j_d}}$, whose time derivative yields:

$$\dot{Q} = \dot{\boldsymbol{q}}_{\boldsymbol{fb}}^T\mathbf{M_{fb}}\ddot{\boldsymbol{q}}_{\boldsymbol{fb}} + \tfrac{1}{2}\dot{\boldsymbol{q}}_{\boldsymbol{fb}}^T\dot{\mathbf{M}}_{\mathbf{fb}}\dot{\boldsymbol{q}}_{\boldsymbol{fb}} + \dot{\boldsymbol{q}}_{\boldsymbol{j}}^T\mathbf{K_P}\boldsymbol{q}_{\boldsymbol{j_{EI}}}, \qquad (4)$$

Substituting the closed-loop equations into (4), produces:

$$\dot{Q} = \dot{\boldsymbol{q}}_{\boldsymbol{fb}}^T\left(\begin{bmatrix}\mathbf{0}\\ \mathbf{K_P}\boldsymbol{q}_{\boldsymbol{j_E}} - \mathbf{K_D}\dot{\boldsymbol{q}}_{\boldsymbol{j}} + \mathbf{M_{jb}}g\boldsymbol{S_s} + \boldsymbol{\nu_P}\left(\dot{\boldsymbol{q}}_{\boldsymbol{b}}^T\mathbf{M_{bb}}g\boldsymbol{S_s}\right)\end{bmatrix} + \begin{bmatrix}\mathbf{J}_{\mathbf{c_b}}^{\mathrm{T}}\boldsymbol{f_p}\\ \mathbf{J}_{\mathbf{c_j}}^{\mathrm{T}}\boldsymbol{f_p}\end{bmatrix} - \mathbf{C_{fb}}\dot{\boldsymbol{q}}_{\boldsymbol{fb}} - \boldsymbol{G}_{\boldsymbol{fb}}\right) + \frac{\dot{\boldsymbol{q}}_{\boldsymbol{fb}}^T\dot{\mathbf{M}}_{\mathbf{fb}}\dot{\boldsymbol{q}}_{\boldsymbol{fb}}}{2} + \dot{\boldsymbol{q}}_{\boldsymbol{j}}^T\mathbf{K_P}\boldsymbol{q}_{\boldsymbol{j_{EI}}}. \qquad (5)$$

Since $\dot{\boldsymbol{q}}_{\boldsymbol{fb}}^T\left(\dot{\mathbf{M}}_{\mathbf{fb}} - 2\mathbf{C_{fb}}\right)\dot{\boldsymbol{q}}_{\boldsymbol{fb}} = 0$ [31][32], and $\dot{\boldsymbol{q}}_{\boldsymbol{j}}^T\boldsymbol{\nu_P} = 1$ (or 0), then direct cancellation of terms leads to the result:

$$\dot{Q} = -\dot{\boldsymbol{q}}_{\boldsymbol{j}}^{T}\mathbf{K_D}\dot{\boldsymbol{q}}_{\boldsymbol{j}} + \dot{\boldsymbol{q}}_{\boldsymbol{fb}}^{T}\begin{bmatrix}\mathbf{J}_{\mathbf{c_b}}^{\mathbf{T}}\boldsymbol{f_p}\\ \mathbf{J}_{\mathbf{c_j}}^{\mathbf{T}}\boldsymbol{f_p}\end{bmatrix}. \quad (6)$$

which consequently satisfies the passivity relationship [33]:

$$\dot{Q} = -\dot{\boldsymbol{q}}_{\boldsymbol{j}}^{T}\mathbf{K_D}\dot{\boldsymbol{q}}_{\boldsymbol{j}} + \dot{\boldsymbol{q}}_{\boldsymbol{fb}}^{T}\begin{bmatrix}\mathbf{J}_{\mathbf{c_b}}^{\mathbf{T}}\boldsymbol{f_p}\\ \mathbf{J}_{\mathbf{c_j}}^{\mathbf{T}}\boldsymbol{f_p}\end{bmatrix} \leq \dot{\boldsymbol{q}}_{\boldsymbol{fb}}^{T}\begin{bmatrix}\mathbf{J}_{\mathbf{c_b}}^{\mathbf{T}}\boldsymbol{f_p}\\ \mathbf{J}_{\mathbf{c_j}}^{\mathbf{T}}\boldsymbol{f_p}\end{bmatrix}. \quad (7)$$

This confirms that only a limited amount of energy can be extracted from the system [33]. To realise closed-loop stability however, one should incorporate force compensation terms into the control scheme, as per the law:

$$\begin{aligned}\boldsymbol{\tau_m} = \mathbf{K_P}\boldsymbol{q}_{\boldsymbol{j_E}} - \mathbf{K_D}\dot{\boldsymbol{q}}_{\boldsymbol{j}} + \mathbf{M_{jb}}g\boldsymbol{S_s} - \mathbf{J}_{\mathbf{c_j}}^{\mathbf{T}}\boldsymbol{f_p}\\ +\boldsymbol{\nu_P}\big(\dot{\boldsymbol{q}}_{\boldsymbol{b}}^{T}\mathbf{M_{bb}}g\boldsymbol{S_s} - \dot{\boldsymbol{q}}_{\boldsymbol{b}}^{T}\mathbf{J}_{\mathbf{c_b}}^{\mathbf{T}}\boldsymbol{f_p}\big),\end{aligned} \quad (8)$$

which contains the $\boldsymbol{f_p}$ vector.

Theorem 2: Implementing controller (8) onto (1), yields a closed-loop system with a Globally Asymptotically Stable (GAS) equilibrium at $\begin{bmatrix}\dot{\boldsymbol{q}}_{\boldsymbol{fb}}^{T} & \boldsymbol{q}_{\boldsymbol{j_E}}^{T}\end{bmatrix} = [\mathbf{0} \quad \mathbf{0}]$.

Proof 2: Equation (3) may be employed as a Lyapunov function, whose time derivative simplifies to:

$$\dot{V} = -\dot{\boldsymbol{q}}_{\boldsymbol{j}}^{T}\mathbf{K_D}\dot{\boldsymbol{q}}_{\boldsymbol{j}} \leq 0, \quad (9)$$

which does prove a form of stability, even though it is devoid of the full state space and/or equilibria. Thus, an altered controller of the following form is introduced:

$$\begin{aligned}\boldsymbol{\tau_m} = \mathbf{K_P}\boldsymbol{q}_{\boldsymbol{j_E}} - \mathbf{K_D}\dot{\boldsymbol{q}}_{\boldsymbol{j}} + \mathbf{M_{jb}}g\boldsymbol{S_s} - \mathbf{J}_{\mathbf{c_j}}^{\mathbf{T}}\boldsymbol{f_p}\\ +\boldsymbol{\nu_P}\big(\dot{\boldsymbol{q}}_{\boldsymbol{b}}^{T}\mathbf{M_{bb}}g\boldsymbol{S_s} - \dot{\boldsymbol{q}}_{\boldsymbol{b}}^{T}\mathbf{J}_{\mathbf{c_b}}^{\mathbf{T}}\boldsymbol{f_p} - a_f - a_j\big),\end{aligned} \quad (10)$$

where $a_f = \dot{\boldsymbol{q}}_{\boldsymbol{b}}^{T}\mathbf{K_F}\dot{\boldsymbol{q}}_{\boldsymbol{b}}$, $a_j = \boldsymbol{q}_{\boldsymbol{j_E}}^{T}\mathbf{K_J}\boldsymbol{q}_{\boldsymbol{j_E}}$, with $\mathbf{K_F} \in \mathbb{R}^{6\times6}$, $\mathbf{K_J} \in \mathbb{R}^{n\times n}$ denoting positive, diagonal matrices of infinitesimal elements. Applying (10) to (1), and using (4), produces:

$$\dot{V} = -\dot{\boldsymbol{q}}_{\boldsymbol{j}}^{T}\mathbf{K_D}\dot{\boldsymbol{q}}_{\boldsymbol{j}} - a_f - a_j \leq 0. \quad (11)$$

Hence, $\dot{V}$ vanishes only when $\dot{\boldsymbol{q}}_{\boldsymbol{fb}} = \boldsymbol{q}_{\boldsymbol{j_E}} = \mathbf{0}$, which implies that the closed-loop system's equilibrium is GAS.

C. Passive Tracking Control of Floating-base Systems

For the purpose of executing locomotion tasks, it is critical to design a control system that is capable of tracking user-defined trajectories (i.e. $\boldsymbol{q}_{\boldsymbol{j_d}} = \boldsymbol{q}_{\boldsymbol{j_d}}(t)$), whilst preserving passivity. To this end, the following control law is proposed:

$$\begin{aligned}\boldsymbol{\tau_m} = \mathbf{K_P}\boldsymbol{q}_{\boldsymbol{j_E}} - \mathbf{K_D}\dot{\boldsymbol{q}}_{\boldsymbol{j}} + \mathbf{M_{jb}}g\boldsymbol{S_s}\\ +\boldsymbol{\nu_P}\big(\dot{\boldsymbol{q}}_{\boldsymbol{b}}^{T}\mathbf{M_{bb}}g\boldsymbol{S_s} - \dot{\boldsymbol{q}}_{\boldsymbol{j_d}}^{T}\mathbf{K_P}\boldsymbol{q}_{\boldsymbol{j_E}}\big).\end{aligned} \quad (12)$$

Theorem 3: Implementing controller (12) onto the dynamical system described by (1), yields a passive system.

Proof 3: Considering the storage function:

$$Q = \tfrac{1}{2}\dot{\boldsymbol{q}}_{\boldsymbol{fb}}^{T}\mathbf{M_{fb}}\dot{\boldsymbol{q}}_{\boldsymbol{fb}} + \tfrac{1}{2}\boldsymbol{q}_{\boldsymbol{j_E}}^{T}\mathbf{K_P}\boldsymbol{q}_{\boldsymbol{j_E}}, \quad (13)$$

and acquiring its time derivative, yields:

$$\begin{aligned}\dot{Q} = \dot{\boldsymbol{q}}_{\boldsymbol{fb}}^{T}\Bigg(\begin{bmatrix}\mathbf{0}\\ \mathbf{K_P}\boldsymbol{q}_{\boldsymbol{j_E}} - \mathbf{K_D}\dot{\boldsymbol{q}}_{\boldsymbol{j}} + \mathbf{M_{jb}}g\boldsymbol{S_s} + \boldsymbol{\nu_s}\end{bmatrix}\\ + \frac{\dot{\mathbf{M}}_{\mathbf{fb}}\dot{\boldsymbol{q}}_{\boldsymbol{fb}}}{2} + \begin{bmatrix}\mathbf{J}_{\mathbf{c_b}}^{\mathbf{T}}\boldsymbol{f_p}\\ \mathbf{J}_{\mathbf{c_j}}^{\mathbf{T}}\boldsymbol{f_p}\end{bmatrix} - \mathbf{C_{fb}}\dot{\boldsymbol{q}}_{\boldsymbol{fb}} - \boldsymbol{G}_{\boldsymbol{fb}}\Bigg) + \dot{\boldsymbol{q}}_{\boldsymbol{j_E}}^{T}\mathbf{K_P}\boldsymbol{q}_{\boldsymbol{j_E}}.\end{aligned} \quad (14)$$

where $\boldsymbol{\nu_s} = \boldsymbol{\nu_P}\big(\dot{\boldsymbol{q}}_{\boldsymbol{b}}^{T}\mathbf{M_{bb}}g\boldsymbol{S_s} - \dot{\boldsymbol{q}}_{\boldsymbol{j_d}}^{T}\mathbf{K_P}\boldsymbol{q}_{\boldsymbol{j_E}}\big)$. Performing the relevant eliminations produces equation (7), thereby leading to satisfaction of the passivity conditions [33].

D. Stable Tracking Control of Floating-base Systems

Despite its ability to maintain closed-loop passivity, the previously presented controller fails to mathematically guarantee stable tracking. To this end, force compensation terms should be incorporated into a control law of the form:

$$\begin{aligned}\boldsymbol{\tau_m} = \mathbf{K_P}\boldsymbol{q}_{\boldsymbol{j_E}} - \mathbf{K_D}\dot{\boldsymbol{q}}_{\boldsymbol{j}} + \mathbf{M_{jb}}g\boldsymbol{S_s} - \mathbf{J}_{\mathbf{c_j}}^{\mathbf{T}}\boldsymbol{f_p} + \boldsymbol{\nu_P}\big(-\dot{\boldsymbol{q}}_{\boldsymbol{b}}^{T}\mathbf{J}_{\mathbf{c_b}}^{\mathbf{T}}\boldsymbol{f_p}\\ -\dot{\boldsymbol{q}}_{\boldsymbol{j_d}}^{T}\mathbf{K_P}\boldsymbol{q}_{\boldsymbol{j_E}} - a_f - a_j + \dot{\boldsymbol{q}}_{\boldsymbol{b}}^{T}\mathbf{M_{bb}}g\boldsymbol{S_s}\big).\end{aligned} \quad (15)$$

Theorem 4: Implementing controller (15) onto the system described by (1), produces a closed-loop system with a GAS equilibrium at $\begin{bmatrix}\dot{\boldsymbol{q}}_{\boldsymbol{fb}}^{T} & \boldsymbol{q}_{\boldsymbol{j_E}}^{T}\end{bmatrix} = [\mathbf{0} \quad \mathbf{0}]$.

Proof 4: Using equation (13) as a Lyapunov function candidate, and performing steps similar to those outlined previously (Proof 3), gives rise to the equation:

$$\begin{aligned}\dot{V} = \dot{\boldsymbol{q}}_{\boldsymbol{fb}}^{T}\Bigg(\begin{bmatrix}\mathbf{0}\\ \mathbf{K_P}\boldsymbol{q}_{\boldsymbol{j_E}} - \mathbf{K_D}\dot{\boldsymbol{q}}_{\boldsymbol{j}} + \mathbf{M_{jb}}g\boldsymbol{S_s} - \mathbf{J}_{\mathbf{c_j}}^{\mathbf{T}}\boldsymbol{f_p} + \boldsymbol{\nu_P}\big(-a_f\\ -a_j + \dot{\boldsymbol{q}}_{\boldsymbol{b}}^{T}\mathbf{M_{bb}}g\boldsymbol{S_s} - \dot{\boldsymbol{q}}_{\boldsymbol{j_d}}^{T}\mathbf{K_P}\boldsymbol{q}_{\boldsymbol{j_E}} - \dot{\boldsymbol{q}}_{\boldsymbol{b}}\mathbf{J}_{\mathbf{c_b}}^{\mathbf{T}}\boldsymbol{f_p}\big)\end{bmatrix}\\ + \begin{bmatrix}\mathbf{J}_{\mathbf{c_b}}^{\mathbf{T}}\boldsymbol{f_p}\\ \mathbf{J}_{\mathbf{c_j}}^{\mathbf{T}}\boldsymbol{f_p}\end{bmatrix} - \begin{bmatrix}\mathbf{M_{bb}}g\boldsymbol{S_s}\\ \mathbf{M_{jb}}g\boldsymbol{S_s}\end{bmatrix}\Bigg) + \dot{\boldsymbol{q}}_{\boldsymbol{j_d}}^{T}\mathbf{K_P}\boldsymbol{q}_{\boldsymbol{j_E}} - \dot{\boldsymbol{q}}_{\boldsymbol{j}}^{T}\mathbf{K_P}\boldsymbol{q}_{\boldsymbol{j_E}},\end{aligned} \quad (16)$$

Further simplifications lead to equation (11), although given that this system is nonautonomous (owing to the time-varying trajectory), substitution of $\dot{V}$'s states directly into the closed-loop system is prohibited. Barbalat's Lemma (BL) is a classical technique for analysing nonautonomous system stability. In this case however, $\boldsymbol{\tau_m}$'s continuity is dubious (due to its possession of $\boldsymbol{\nu_P}$), which could preclude BL's applicability. Nonetheless, one may apply the 'new Invariance Principle' (NIP) [34], by considering that the closed-loop system is of the form $\dot{\boldsymbol{x}}_{\boldsymbol{F}} = f(\boldsymbol{x}_{\boldsymbol{F}}, t)$ [34], i.e.:

$$\ddot{\boldsymbol{q}}_{\boldsymbol{fb}} = \mathbf{M}_{\mathbf{fb}}^{-\mathbf{1}}\left(\begin{bmatrix}\mathbf{0}\\ \boldsymbol{\tau_m}\end{bmatrix} + \begin{bmatrix}\mathbf{J}_{\mathbf{c_b}}^{\mathbf{T}}\boldsymbol{f_p}\\ \mathbf{J}_{\mathbf{c_j}}^{\mathbf{T}}\boldsymbol{f_p}\end{bmatrix} - \boldsymbol{G}_{\boldsymbol{fb}} - \mathbf{C_{fb}}\dot{\boldsymbol{q}}_{\boldsymbol{fb}}\right). \quad (17)$$

[34] proves that the state, $\boldsymbol{x}_{\boldsymbol{F}} = \begin{bmatrix}\dot{\boldsymbol{q}}_{\boldsymbol{fb}}^{T} & \boldsymbol{q}_{\boldsymbol{fb}}^{T}\end{bmatrix}^{\boldsymbol{T}}$, is bounded, if $V > 0$ and $\dot{V} \leq 0$. Moreover, discontinuous input signals do

not impinge on stability, if $V > 0$ and $\dot{V} \leq 0$ [34], provided that there exists a function, W, such that:

$$\dot{V} = -\dot{\boldsymbol{q}}_{\boldsymbol{j}}^{\boldsymbol{T}}\mathbf{K_D}\dot{\boldsymbol{q}}_{\boldsymbol{j}} - a_f - a_j < W \leq 0, \quad (18)$$

where $W = -\boldsymbol{q}_{\boldsymbol{w}}^{\boldsymbol{T}}\boldsymbol{\Omega}\boldsymbol{q}_{\boldsymbol{w}}$, with $\boldsymbol{\Omega} > \mathbf{0}$ and $\boldsymbol{q}_{\boldsymbol{w}} = \left[\dot{\boldsymbol{q}}_{\boldsymbol{fb}}^{\boldsymbol{T}}\ \boldsymbol{q}_{\boldsymbol{j_E}}^{\boldsymbol{T}}\right]^{\boldsymbol{T}}$. Assuming that $\mathbf{K_F}$ and $\mathbf{K_J}$ are varied in real-time, differentiating W produces the function:

$$\dot{W} = -2\boldsymbol{q}_{\boldsymbol{w}}^{\boldsymbol{T}}\boldsymbol{\Omega}\dot{\boldsymbol{q}}_{\boldsymbol{w}} - \boldsymbol{q}_{\boldsymbol{w}}^{\boldsymbol{T}}\dot{\boldsymbol{\Omega}}\boldsymbol{q}_{\boldsymbol{w}}. \quad (19)$$

Since $\dot{W} = 0$ at $\boldsymbol{q}_{\boldsymbol{w}} = \mathbf{0}$, then $\dot{V} \equiv 0$ (identically zero). Differentiating once more, yields the following expression:

$$\ddot{W} = -2\dot{\boldsymbol{q}}_{\boldsymbol{w}}^{\boldsymbol{T}}\boldsymbol{\Omega}\dot{\boldsymbol{q}}_{\boldsymbol{w}} - 2\boldsymbol{q}_{\boldsymbol{w}}^{\boldsymbol{T}}\boldsymbol{\Omega}\ddot{\boldsymbol{q}}_{\boldsymbol{w}} - 4\boldsymbol{q}_{\boldsymbol{w}}^{\boldsymbol{T}}\dot{\boldsymbol{\Omega}}\dot{\boldsymbol{q}}_{\boldsymbol{w}} - \boldsymbol{q}_{\boldsymbol{w}}^{\boldsymbol{T}}\ddot{\boldsymbol{\Omega}}\boldsymbol{q}_{\boldsymbol{w}}, \quad (20)$$

which is only nullified at $\boldsymbol{q}_{\boldsymbol{w}} = \dot{\boldsymbol{q}}_{\boldsymbol{w}} = \mathbf{0}$. In view of the fact that $\boldsymbol{q}_{\boldsymbol{w}} \equiv 0$, and the system's states are bounded, while $\dot{V} \equiv 0$ and contains the equilibria, then in accordance with the NIP [34] this nonautonomous system asymptotically converges to the $\boldsymbol{q}_{\boldsymbol{w}}$ equilibrium, and is therefore GAS.

III. Model-Free Control of Floating-Base Robots

A. Decoupled Dynamics via Coordinate Transformation

The direct coupling between floating-base and joint-space coordinates that is observed in model (1), could be expunged by following the approach outlined in [18], which yields the model provided below:

$$\begin{bmatrix}\mathbf{M_{br}} & \mathbf{0}\\ \mathbf{0} & \mathbf{M_{jj}}\end{bmatrix}\ddot{\boldsymbol{q}}_{\boldsymbol{fd}} + \begin{bmatrix}\mathbf{0}\\ \mathbf{C}\end{bmatrix} + \begin{bmatrix}\mathbf{M_{br}}g\boldsymbol{S_c}\\ \mathbf{0}\end{bmatrix} = \begin{bmatrix}\mathbf{0}\\ \boldsymbol{\tau_m}\end{bmatrix} - \begin{bmatrix}\mathbf{I}\\ \mathbf{J_c^T}\end{bmatrix}\boldsymbol{f}_{\boldsymbol{g}}, \quad (21)$$

where $\boldsymbol{S_c} = [0\ \ 0\ \ 1]^{\boldsymbol{T}}$, $\ddot{\boldsymbol{q}}_{\boldsymbol{fd}} \in \mathbb{R}^{n+3} = \left[\ddot{\boldsymbol{q}}_{\boldsymbol{c}}^{\boldsymbol{T}}\ \ \ddot{\boldsymbol{q}}_{\boldsymbol{j}}^{\boldsymbol{T}}\right]^{\boldsymbol{T}}$, with $\ddot{\boldsymbol{q}}_{\boldsymbol{c}} \in \mathbb{R}^3$ denoting the Centre-of-Mass (CoM) coordinates, $\mathbf{C} \in \mathbb{R}^n = \mathbf{C}(\boldsymbol{q}_{\boldsymbol{j}}, \dot{\boldsymbol{q}}_{\boldsymbol{j}})\dot{\boldsymbol{q}}_{\boldsymbol{j}}$ representing the Coriolis and centrifugal terms matrix, $\mathbf{J_c^T} \in \mathbb{R}^{n\times 3}$ symbolising the CoM to contact-point Jacobian, and $\boldsymbol{f}_{\boldsymbol{g}} \in \mathbb{R}^3$ signifying the Gross Applied Force (GAF), as depicted in Fig. 2. The inertia matrix $\mathbf{M_{fd}} \in \mathbb{R}^{(n+3)\times(n+3)} = diag(\mathbf{M_{br}}, \mathbf{M_{jj}})$, with $\mathbf{M_{br}} = diag(m, m, m)$. This model also possesses the $\dot{\boldsymbol{q}}_{\boldsymbol{j}}^{\boldsymbol{T}}(\dot{\mathbf{M}}_{\mathbf{jj}} - 2\mathbf{C})\dot{\boldsymbol{q}}_{\boldsymbol{j}} = 0$ property [31][32][35], and for simplicity, it considers solely the 3 translational CoM coordinates [18].

B. Passive Model-Free Control of Legged Robots

In view of the uncoupled dynamical model shown above, it is possible to define the following passivating control law:

$$\boldsymbol{\tau_m} = \mathbf{K_P}\boldsymbol{q}_{\boldsymbol{j_E}} - \mathbf{K_D}\dot{\boldsymbol{q}}_{\boldsymbol{j}} + \boldsymbol{\nu_P}(\dot{\boldsymbol{q}}_{\boldsymbol{c}}^{\boldsymbol{T}}\mathbf{M_{br}}g\boldsymbol{S_c}), \quad (22)$$

which obviates the need for model-based terms.

Theorem 5: Implementing controller (22) onto the system described by (21), yields a passive closed-loop system.

Proof 5: Considering the following storage function:

$$Q = \tfrac{1}{2}\dot{\boldsymbol{q}}_{\boldsymbol{fd}}^{\boldsymbol{T}}\mathbf{M_{fd}}\dot{\boldsymbol{q}}_{\boldsymbol{fd}} + \tfrac{1}{2}\boldsymbol{q}_{\boldsymbol{j_E}}^{\boldsymbol{T}}\mathbf{K_P}\boldsymbol{q}_{\boldsymbol{j_E}}, \quad (23)$$

and performing steps similar to those outlined in Proofs 1 to 4, gives rise to the equation:

$$\dot{Q} = -\dot{\boldsymbol{q}}_{\boldsymbol{j}}^{\boldsymbol{T}}\mathbf{K_D}\dot{\boldsymbol{q}}_{\boldsymbol{j}} - \dot{\boldsymbol{q}}_{\boldsymbol{fd}}^{\boldsymbol{T}}\begin{bmatrix}\boldsymbol{f}_{\boldsymbol{g}}\\ \mathbf{J_c^T}\boldsymbol{f}_{\boldsymbol{g}}\end{bmatrix} \leq -\dot{\boldsymbol{q}}_{\boldsymbol{fd}}^{\boldsymbol{T}}\begin{bmatrix}\boldsymbol{f}_{\boldsymbol{g}}\\ \mathbf{J_c^T}\boldsymbol{f}_{\boldsymbol{g}}\end{bmatrix}, \quad (24)$$

thus satisfying the conditions for passivity [33].

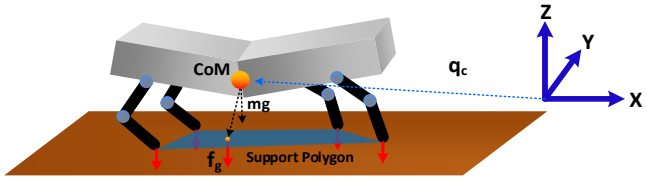

Figure 2. Schematic of a metamorphic quadrupedal floating-base robot.

However, controller (22)'s energy efficiency could be ameliorated via the following control law:

$$\boldsymbol{\tau_m} = \mathbf{K_P}\boldsymbol{q}_{\boldsymbol{j_E}} - \mathbf{K_D}\dot{\boldsymbol{q}}_{\boldsymbol{j}} + \boldsymbol{\nu_P}(\dot{\boldsymbol{q}}_{\boldsymbol{c}}^{\boldsymbol{T}}\boldsymbol{f}_{\boldsymbol{g}} + \dot{\boldsymbol{q}}_{\boldsymbol{c}}^{\boldsymbol{T}}\mathbf{M_{br}}g\boldsymbol{S_c}), \quad (25)$$

for the array of reasons outlined in sub-section III. D. Implementation of the above scheme, yields the relationship:

$$\dot{Q} = -\dot{\boldsymbol{q}}_{\boldsymbol{j}}^{\boldsymbol{T}}\mathbf{K_D}\dot{\boldsymbol{q}}_{\boldsymbol{j}} - \dot{\boldsymbol{q}}_{\boldsymbol{j}}^{\boldsymbol{T}}\mathbf{J_c^T}\boldsymbol{f}_{\boldsymbol{g}} \leq -\dot{\boldsymbol{q}}_{\boldsymbol{j}}^{\boldsymbol{T}}\mathbf{J_c^T}\boldsymbol{f}_{\boldsymbol{g}}, \quad (26)$$

thereby attesting to passivity of the closed-loop system.

C. Stable Model-Free Tracking Control of Legged Robots

A stable control design could be produced in a similar model-free fashion to that previously delineated, although in this case, compensation of force terms is necessary for convergence. Thus, the following control law is proposed:

$$\begin{aligned}\boldsymbol{\tau_m} &= \mathbf{K_P}\boldsymbol{q}_{\boldsymbol{j_E}} - \mathbf{K_D}\dot{\boldsymbol{q}}_{\boldsymbol{j}} + \mathbf{J_c^T}\boldsymbol{f}_{\boldsymbol{g}}\\ &+\boldsymbol{\nu_P}(\dot{\boldsymbol{q}}_{\boldsymbol{c}}^{\boldsymbol{T}}\boldsymbol{f}_{\boldsymbol{g}} + \dot{\boldsymbol{q}}_{\boldsymbol{c}}^{\boldsymbol{T}}\mathbf{M_{br}}g\boldsymbol{S_c} - \dot{\boldsymbol{q}}_{\boldsymbol{j_d}}^{\boldsymbol{T}}\mathbf{K_P}\boldsymbol{q}_{\boldsymbol{j_E}} - a_c),\end{aligned} \quad (27)$$

where $a_c = \dot{\boldsymbol{q}}_{\boldsymbol{c}}^{\boldsymbol{T}}\mathbf{K_c}\dot{\boldsymbol{q}}_{\boldsymbol{c}}$, with $\mathbf{K_c} \in \mathbb{R}^{3\times 3}$ denoting a diagonal matrix of infinitesimal-valued terms. Since $\mathbf{M_{br}}$ comprises the scalar, total robot mass terms, this scheme is model-free.

Theorem 6: Implementing controller (27) onto (21), yields a GAS closed-loop equilibrium at $\left[\dot{\boldsymbol{q}}_{\boldsymbol{fd}}^{\boldsymbol{T}}\ \boldsymbol{q}_{\boldsymbol{j_E}}^{\boldsymbol{T}}\right] = [\mathbf{0}\ \ \mathbf{0}]$.

Proof 6: Considering the following Lyapunov function:

$$V = \tfrac{1}{2}\dot{\boldsymbol{q}}_{\boldsymbol{fd}}^{\boldsymbol{T}}\mathbf{M_{fd}}\dot{\boldsymbol{q}}_{\boldsymbol{fd}} + \tfrac{1}{2}\boldsymbol{q}_{\boldsymbol{j_E}}^{\boldsymbol{T}}\mathbf{K_P}\boldsymbol{q}_{\boldsymbol{j_E}}, \quad (28)$$

and obtaining its time derivative, while performing simplifications analogous to those previously shown, yields:

$$\dot{V} = \dot{\boldsymbol{q}}_{\boldsymbol{fd}}^{\boldsymbol{T}}\left(\begin{bmatrix}\mathbf{0}\\ \mathbf{K_P}\boldsymbol{q}_{\boldsymbol{j_E}} - \mathbf{K_D}\dot{\boldsymbol{q}}_{\boldsymbol{j}} + \mathbf{J_c^T}\boldsymbol{f}_{\boldsymbol{g}} +\\ \boldsymbol{\nu_P}(\dot{\boldsymbol{q}}_{\boldsymbol{c}}^{\boldsymbol{T}}\boldsymbol{f}_{\boldsymbol{g}} + \dot{\boldsymbol{q}}_{\boldsymbol{c}}^{\boldsymbol{T}}\mathbf{M_{br}}g\boldsymbol{S_c} - \dot{\boldsymbol{q}}_{\boldsymbol{j_d}}^{\boldsymbol{T}}\mathbf{K_P}\boldsymbol{q}_{\boldsymbol{j_E}} - a_c)\end{bmatrix}\right)$$

$$+\frac{1}{2}\dot{\mathbf{M}}_{\mathbf{fd}}\dot{\boldsymbol{q}}_{\boldsymbol{fd}}-\begin{bmatrix}\mathbf{M}_{\mathbf{br}}g\boldsymbol{S}_{\boldsymbol{c}}\\ \mathbf{0}\end{bmatrix}-\begin{bmatrix}\mathbf{0}\\ \mathbf{C}\end{bmatrix}-\begin{bmatrix}\mathbf{I}\\ \mathbf{J}_{\mathbf{c}}^{\mathbf{T}}\end{bmatrix}\boldsymbol{f}_{\boldsymbol{g}}\Big)+\dot{\boldsymbol{q}}_{\boldsymbol{j_E}}^{\boldsymbol{T}}\mathbf{K}_{\mathbf{P}}\boldsymbol{q}_{\boldsymbol{j_E}}, \quad (29)$$

which consequently results in:

$$\dot{V}=-\dot{\boldsymbol{q}}_{\boldsymbol{j}}^{\boldsymbol{T}}\mathbf{K}_{\mathbf{D}}\dot{\boldsymbol{q}}_{\boldsymbol{j}}-a_c\leq 0. \quad (30)$$

Following the approach outlined in Proof 4, which is based on the NIP [34], enables one to conclude that $\dot{\boldsymbol{q}}_{\boldsymbol{fd}}$ tends to zero. In order to prove GAS however, the zero states of $\dot{V}$ are substituted into the closed-loop dynamics, producing:

$$\begin{bmatrix}\mathbf{M}_{\mathbf{br}}g\boldsymbol{S}_{\boldsymbol{c}}\\ \mathbf{0}\end{bmatrix}=\begin{bmatrix}\mathbf{0}\\ \mathbf{K}_{\mathbf{P}}\boldsymbol{q}_{\boldsymbol{j_E}}\end{bmatrix}-\begin{bmatrix}\mathbf{I}\\ \mathbf{0}\end{bmatrix}\boldsymbol{f}_{\boldsymbol{g}}, \quad (31)$$

which implies that $\boldsymbol{q}_{\boldsymbol{j_E}}=\mathbf{0}$. One may then state that:

$$[0\quad 0\quad mg]^T=-\boldsymbol{f}_{\boldsymbol{g}}, \quad (32)$$

$$[0\quad 0\quad mg]^T=-[f_x\quad f_y\quad f_z]^T, \quad (33)$$

thus revealing that $f_x=f_y=0$, and $f_z=-mg$. Hence, $\left[\dot{\boldsymbol{q}}_{\boldsymbol{fd}}^{\boldsymbol{T}}\,\boldsymbol{q}_{\boldsymbol{j_E}}^{\boldsymbol{T}}\right]=[\mathbf{0}\quad\mathbf{0}]$ is the largest invariant set, around which the equilibrium point is GAS. For a more direct proof, one could append a_j to the PSS of (27), which would produce (11), and the conclusion that since all the equilibria are contained in $\dot{V}$, then the system is GAS. The presented controller constitutes a straightforwardly implementable, fully model-free control scheme, which provably converges to the desired equilibria during execution of tracking tasks.

D. Controller Feasibility Discussion

Unfeasible control signals may arise when $\dot{\boldsymbol{q}}_{\boldsymbol{j_i}}\approx\mathbf{0}$, since $\mathbf{M}_{\mathbf{br}}g$ inherently possesses a large magnitude. Thus, it is preferable to employ the control schemes that contain measured or estimated external force elements, given that:

$$\dot{\boldsymbol{q}}_{\boldsymbol{c}}^{\boldsymbol{T}}\left(\mathbf{M}_{\mathbf{br}}g\boldsymbol{S}_{\boldsymbol{c}}+\boldsymbol{f}_{\boldsymbol{g}}\right)=-\dot{\boldsymbol{q}}_{\boldsymbol{c}}^{\boldsymbol{T}}\mathbf{M}_{\mathbf{br}}\ddot{\boldsymbol{q}}_{\boldsymbol{c}}=-m(\dot{x}\ddot{x}+\dot{y}\ddot{y}+\dot{z}\ddot{z}), \quad (34)$$

where the vertical acceleration, $\ddot{z}$, is typically deemed a negligible quantity [11][36], thus reducing the equation to:

$$\dot{\boldsymbol{q}}_{\boldsymbol{c}}^{\boldsymbol{T}}\left(\mathbf{M}_{\mathbf{br}}g\boldsymbol{S}_{\boldsymbol{c}}+\boldsymbol{f}_{\boldsymbol{g}}\right)=-\dot{\boldsymbol{q}}_{\boldsymbol{c}}^{\boldsymbol{T}}\mathbf{M}_{\mathbf{br}}\ddot{\boldsymbol{q}}_{\boldsymbol{c}}=-m(\dot{x}\ddot{x}+\dot{y}\ddot{y}). \quad (35)$$

Interestingly, saturation can always be prevented when $\dot{\boldsymbol{q}}_{\boldsymbol{c}}^{\boldsymbol{T}}\left(\mathbf{M}_{\mathbf{br}}g\boldsymbol{S}_{\boldsymbol{c}}+\boldsymbol{f}_{\boldsymbol{g}}\right)-\dot{\boldsymbol{q}}_{\boldsymbol{j_d}}^{\boldsymbol{T}}\mathbf{K}_{\mathbf{P}}\boldsymbol{q}_{\boldsymbol{j_E}}>0$, by using the controller:

$$\boldsymbol{\tau}_{\boldsymbol{m}}=\mathbf{K}_{\mathbf{P}}\boldsymbol{q}_{\boldsymbol{j_E}}-\mathbf{K}_{\mathbf{D}}\dot{\boldsymbol{q}}_{\boldsymbol{j}}+\mathbf{J}_{\mathbf{c}}^{\mathbf{T}}\boldsymbol{f}_{\boldsymbol{g}}+\boldsymbol{\nu}_{\boldsymbol{P}}(f_v-p_s), \quad (36)$$

where $f_v=\dot{\boldsymbol{q}}_{\boldsymbol{c}}^{\boldsymbol{T}}\left(\mathbf{M}_{\mathbf{br}}g\boldsymbol{S}_{\boldsymbol{c}}+\boldsymbol{f}_{\boldsymbol{g}}\right)-\dot{\boldsymbol{q}}_{\boldsymbol{j_d}}^{\boldsymbol{T}}\mathbf{K}_{\mathbf{P}}\boldsymbol{q}_{\boldsymbol{j_E}}-a_c-a_j$, and p_s denotes an arbitrarily large, user-regulated positive constant, whose aim is to suppress the portion of the control signal that is multiplied by $\boldsymbol{\nu}_{\boldsymbol{P}}$. This is permissible, since addition of an arbitrarily large negative value, would lead to:

$$\dot{V}=-\dot{\boldsymbol{q}}_{\boldsymbol{j}}^{\boldsymbol{T}}\mathbf{K}_{\mathbf{D}}\dot{\boldsymbol{q}}_{\boldsymbol{j}}-a_c-a_j-p_s\leq 0, \quad (37)$$

thereby preserving stability. Obversely, when $f_v<0$, addition of an arbitrarily large, positive p_s value, may lead to violation of (37). It is however possible to perform stiffness modulations [37]-[39], which will have no bearing on $\dot{V}$ [29], provided that $p_s=c\cdot\boldsymbol{q}_{\boldsymbol{j_E}}^{\boldsymbol{T}}\dot{\mathbf{K}}_{\mathbf{P}}\boldsymbol{q}_{\boldsymbol{j_E}}$, with c denoting a positive constant. To ensure that $f_v-p_s\geq 0$, when $f_v<0$, it is mandatory to decrease the stiffness values, such that $\dot{\mathbf{K}}_{\mathbf{P}}<0$, which would yield $f_v+p_s\geq 0$. The objective is to then satisfy the following relationship:

$$f_v+p_s=s_{\boldsymbol{c}}, \quad (38)$$

where $s_{\boldsymbol{c}}$ is a user-defined variable that when multiplied by $\|\boldsymbol{\nu}_{\boldsymbol{P}}\|$, yields τ_{m_r}; a feasible input signal. It is assumed that all $\mathbf{K}_{\mathbf{P}}$ gains are modulated at the same rate, such that:

$$\boldsymbol{q}_{\boldsymbol{j_E}}^{\boldsymbol{T}}\dot{\mathbf{K}}_{\mathbf{P}}\boldsymbol{q}_{\boldsymbol{j_E}}=c\cdot\boldsymbol{q}_{\boldsymbol{j_E}}^{\boldsymbol{T}}\mathbf{I}\boldsymbol{q}_{\boldsymbol{j_E}}\geq f_v. \quad (39)$$

The active stiffness gains should then be modulated at a rate determined by the following variable:

$$c=f_v\cdot\left(\boldsymbol{q}_{\boldsymbol{j_E}}^{\boldsymbol{T}}\mathbf{I}\boldsymbol{q}_{\boldsymbol{j_E}}\right)^{+}. \quad (40)$$

In practice, exceedingly large $\boldsymbol{q}_{\boldsymbol{j_E}}^{\boldsymbol{T}}\dot{\mathbf{K}}_{\mathbf{P}}\boldsymbol{q}_{\boldsymbol{j_E}}$ magnitudes are attainable, since $\mathbf{K}_{\mathbf{P}}$ can be modulated aggressively, thus leading to production of values eclipsing $\dot{\boldsymbol{q}}_{\boldsymbol{j_d}}^{\boldsymbol{T}}\mathbf{K}_{\mathbf{P}}\boldsymbol{q}_{\boldsymbol{j_E}}$. The $\mathbf{K}_{\mathbf{P}}$ values should be reverted to their original state, once $f_v\geq 0$.

IV. Walking Experiments Using a Metamorphic Quadrupedal Robot

A. Experimental Setup

The Metamorphic Walker (MW) [40] is a 1.2 kg reconfigurable robot capable of switching between various forms, which allows it to mimic mammal and insect gaits. It comprises a total of 14 actuated joints, incorporating 12-bit position encoders. In this work, the MW has been equipped with four Parallax Inc FlexiForce pressure sensors (~0.7 kg resolution), which are used to extract vertical contact force measurements that are then transmitted to an Arduino Uno. Control law (36) is implemented on a custom microcontroller provided by the manufacturer [40]. A Mathworks MATLAB interface enables the user to broadcast commands to the microcontroller, via Bluetooth, thereby triggering a set of predefined actions and gaits.

B. Arachnoid Gait

In order to realise locomotory tasks, control law (36) has been implemented on the robot, as this is the only presented control scheme that yields a GAS closed-loop system, through a model-free approach. $\dot{x}$, $\ddot{x}$, $\dot{y}$, $\ddot{y}$, $\dot{z}$, and $\ddot{z}$ are estimated via numerical differentiation of the forward kinematics relationship, $\dot{\boldsymbol{q}}_{\boldsymbol{c}}=\mathbf{J}_{\mathbf{t}}\dot{\boldsymbol{q}}_{\boldsymbol{j}}$, where $\mathbf{J}_{\mathbf{t}}\in\mathbb{R}^{3\times n}$ denotes a CoM Jacobian. This permits computation of the GAF, via $\mathbf{M}_{\mathbf{br}}\ddot{\boldsymbol{q}}_{\boldsymbol{c}}+\mathbf{M}_{\mathbf{br}}g\boldsymbol{S}_{\boldsymbol{c}}=-\boldsymbol{f}_{\boldsymbol{g}}$. Comparable performance levels are observed, regardless of whether the $\boldsymbol{f}_{\boldsymbol{g}}$ vector is estimated solely via encoder feedback, or calculated from a

combination of encoder and force/pressure sensor readings. The former method is preferable however, as the pressure sensors introduce slippage effects, and their measurement accuracy depends on the nature of the contact. Although

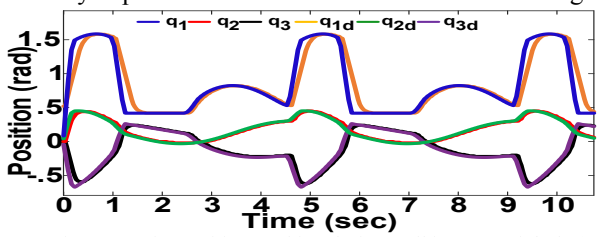

Figure 3. Joint position tracking during walking (rear right leg).

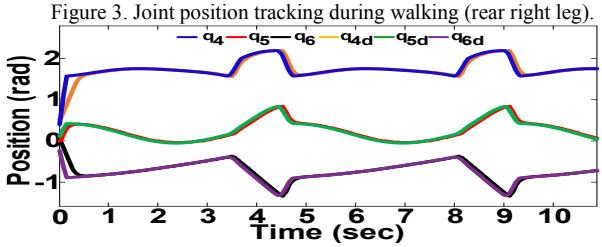

Figure 4. Joint position tracking during walking (front right leg).

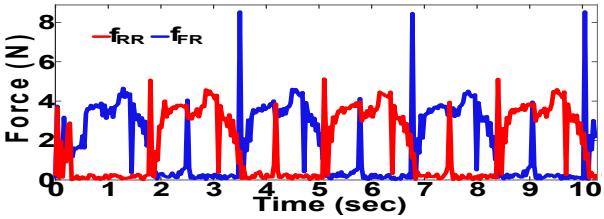

Figure 5. Vertical ground reaction forces during locomotion (right legs).

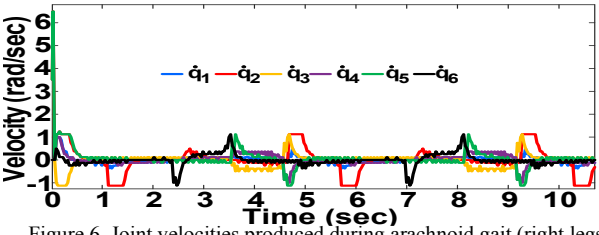

Figure 6. Joint velocities produced during arachnoid gait (right legs).

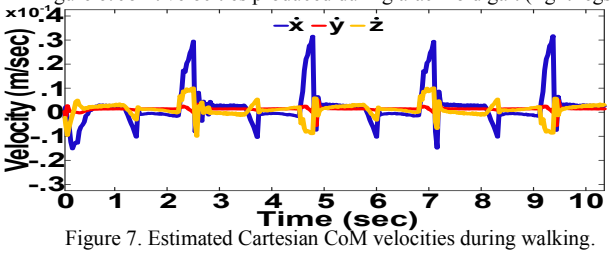

Figure 7. Estimated Cartesian CoM velocities during walking.

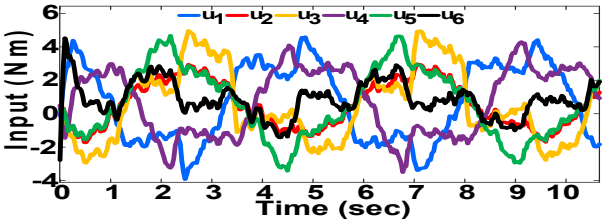

Figure 8. Input signals produced during arachnoid gait (right legs).

slippage effects can be compensated via the PSS, this exceeds the presented work's scope. The controller is supplied with a continuous position trajectory, based on which the desired joint velocities, $\dot{\boldsymbol{q}}_{jd}^{T}$, are computed iteratively. Figs. 3 and 4 display the joint-tracking performance pertaining to the rear-right and front-right legs, during walking. The leg joints are enumerated from 1 to 12, starting from the rear right leg, with joints closest to the robot's body possessing the lowest numbers in every leg chain.

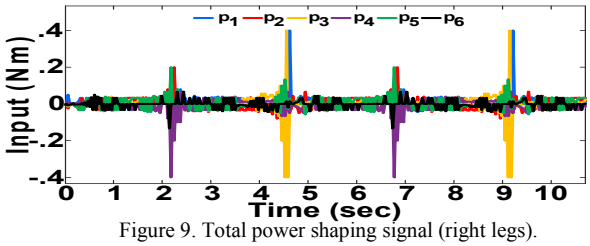

Figure 9. Total power shaping signal (right legs).

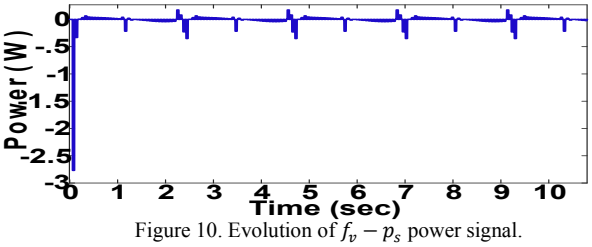

Figure 10. Evolution of $f_v - p_s$ power signal.

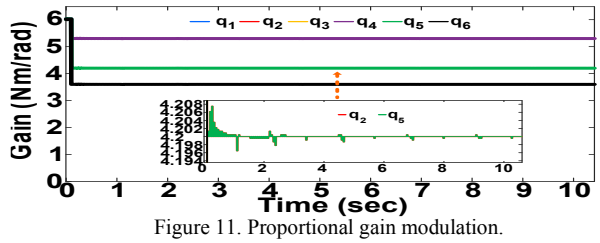

Figure 11. Proportional gain modulation.


Figure 12. MW snapshots with (right) and without (left) pressure sensors.

Moreover, Fig. 5 contains the ground reaction forces measured by the pressure pads (Fig. 12), Fig. 6 illustrates the joint velocity values, and Fig. 7 contains the computed Cartesian CoM velocities. Fig. 8 depicts the input signals, while the various constituents of the overall control signal are displayed in Figs. 9 and 10. To be precise, Fig. 9 plots the total values of $\boldsymbol{\nu_P}(f_v - p_s)$, which are clearly upper bounded, as a result of the previously described $f_v + p_s \approx s_c$ relationship. Fig. 10 displays the scalar $f_v - p_s$ term's real-time evolution, which determines the required, automatic gain modulation presented in Fig. 11 that also includes a magnified plot of $\boldsymbol{q_2}$ and $\boldsymbol{q_5}$'s gains. Videos of the walking experiments are contained within the accompanying file.

V. Conclusion

This work presents an array of designs for stable and passive control of under-actuated, floating-base robots with contacts. The control designs are all founded on one central concept, namely the direct incorporation of PSS terms into the developed control laws, as is also performed in [29][30]. A general floating-base model is initially considered, in conjunction with minimally model-based controllers that can guarantee closed-loop passivity and stability. Subsequently, a decoupled version of the floating-base model is

constructed via coordinate transformation [18]. Utilisation of this tractable mathematical representation enables the creation of model-free controllers, which provably guarantee passivity and tracking stability, for floating-base robots with contacts. A variable impedance control strategy [29][30] is then propounded, to guarantee production of feasible control signals. Experimental results extacted from a reconfigurable quadrupedal robot (MW), corroborate the theoretical analysis and the controller's feasibility.

ACKNOWLEDGEMENT

This work is supported by the EP/S019790/1, and EP/P026087/1 EPSRC grants. The authors would also like to express their gratitude for Mr. Jon West's technical support.

REFERENCES

[1] R. Tedrake, Underactuated Robotics: Algorithms for Walking, Running, Swimming, Flying, and Manipulation (Course Notes for MIT 6.832). Downloaded on 23/10/19 from *http://underactuated.mit.edu/*.

[2] M. Mahvash, P. E. Dupont, "Stiffness control of surgical continuum manipulators," *IEEE Transactions on Robotics,* vol. 27, no. 2, pp. 334-345, 2011.

[3] G. A. Pratt, M. M. Williamson, "Series Elastic Actuators," *IEEE/RSJ International Conference on Intelligent Robots and Systems,* pp. 399-406, 1995.

[4] P. Tomei, "A simple PD controller for robots with elastic joints," *IEEE Transactions on Automatic Control,* vol. 36, no. 10, pp. 1208-1213, 1991.

[5] L. Tian, A. Goldenberg, "Robust Adaptive Control of Flexible Joint Robots with Joint Torque Feedback," *IEEE International Conference on Robotics and Automation,* pp. 1229-1234, 1995.

[6] S. Nicosia, P. Tomei, "Design of Global Tracking Controllers for Flexible-Joint Robots," *Journal of Robotic Systems,* vol. 10, no. 6, pp. 835-846, 1993.

[7] S. Nicosia, P. Tomei, "A Tracking Controller for Flexible-Joint Robots Using Only Link Position Feedback," *IEEE Transactions on Automatic Control,* vol. 40, no. 5, pp. 885-890, 1995.

[8] M. Keppler, D. Lakatos, C. Ott, A. Albu-Schaffer *"*Elastic Structure Preserving (ESP) Control for Compliantly Actuated Robots*," IEEE Transactions on Robotics,* vol. 34, no. 2, pp. 317-335, 2018.

[9] C. Bergeles et al., "Concentric tube robot design and optimization based on task and anatomical constraints," *IEEE Transactions on Robotics,* vol. 31, no. 1, pp. 67-84, 2015.

[10] N. Giri, I. D. Walker, "Three module lumped element model of a continuum arm section," *IEEE/RSJ International Conference on Intelligent Robots and Systems,* pp. 4060-4065, 2011.

[11] S. Kajita, K. Tani, "Study of Dynamic Biped Locomotion on Rugged Terrain – Derivation and Application of the Linear Inverted Pendulum Mode," *IEEE International Conference on Robotics and Automation,* pp. 1405-1411, 1991.

[12] Y. Umetami, K. Yoshida, "Resolved motion rate control of space manipulators with generalized Jacobian matrix," *IEEE Transactions on Robotics and Automation,* vol. 5, no. 3, pp. 303-314, 1989.

[13] E. Papadopoulos, S. Dubowsky, "On the nature of control algorithms for free-floating space manipulators" *IEEE Transactions on Robotics and Automation,* vol. 7, no. 6, pp. 1102-1108, 1991.

[14] S. Dubowsky, E. Papadopoulos, "The kinematics, dynamics, and control of free-flying and free-floating space robotic systems," *IEEE Transactions on Robotics and Automation,* vol. 9, no. 5, pp. 531-543, 1993.

[15] L. Sentis, O. Khatib, "Control of Free-Floating Humanoid Robots Through Task Prioritization," *IEEE International Conference on Robotics and Automation,* pp. 1718–1723, 2005.

[16] J. Park, O. Khatib, "Contact Consistent Control Framework for Humanoid Robots," *IEEE International Conference on Robotics and Automation,* pp. 1963–1969, 2006.

[17] J. Nakanishi, M. Mistry, S. Schaal, "Inverse Dynamics Control with Floating Base and Constraints," *IEEE International Conference on Robotics and Automation,* pp. 1942–1947, 2007.

[18] S. –H. Hyon, J. G. Hale, G. Cheng, "Full-Body Compliant Human-Humanoid Interaction: Balancing in the Presence of Unknown External Forces," *IEEE Transactions on Robotics,* vol. 23, no. 5, pp. 884-898, 2007.

[19] M. Mistry, J. Buchli, S. Schaal, "Inverse Dynamics Control of Floating Base Systems Using Orthogonal Decomposition," *IEEE International Conference on Robotics and Automation,* pp. 3406–3412, 2010.

[20] L. Righetti, J. Buchli, M. Mistry, S. Schaal, "Control of legged robots with optimal distribution of contact forces," *IEEE-RAS International Conference on Humanoid Robots,* pp. 318–324, 2011.

[21] L. Saab et al., "Generic Dynamic Motion Generation with Multiple Unilateral Constraints," *IEEE/RSJ International Conference on Intelligent Robots and Systems,* pp. 4127-4133, 2011.

[22] A. Herzog et al. "Balancing experiments on a torque-controlled humanoid with hierarchical inverse dynamics," *IEEE/RSJ International Conference on Intelligent Robots and Systems,* pp. 981-988, 2014.

[23] B. Henze, M. A. Roa, C. Ott, "Passivity-based whole-body balancing for torque-controlled humanoid robots in multi-contact scenarios," *The International Journal of Robotics Research,* vol. 35, no. 12, pp. 1522-1543, 2016.

[24] S. Mason, N. Rotella, S. Schaal, L. Righetti, "Balancing and Walking Using Full Dynamics LQR Control With Contact Constraints," *IEEE-RAS International Conference on Humanoid Robots,* pp. 63-68, 2016.

[25] E. Spyrakos-Papastavridis et al., "Selective-Compliance-Based Lagrange Model and Multilevel Noncollocated Feedback Control of a Humanoid Robot," *Journal of Mechanisms and Robotics,* vol. 10, no. 3, pp. 031009, 2018.

[26] E. Spyrakos-Papastavridis, D. G. Caldwell, N. G. Tsagarakis, "Balance and Impedance Optimization Control for Compliant Humanoid Stepping," *IEEE/RSJ International Conference on Intelligent Robots and Systems,* pp. 1349-1355, 2016.

[27] J. Buchli et al., "Compliant Quadruped Locomotion Over Rough Terrain," *IEEE/RSJ International Conference on Intelligent Robots and Systems,* pp. 814-820, 2009.

[28] G. Nava et al., "Stability Analysis and Design of Momentum-based Controllers for Humanoid Robots," *IEEE/RSJ International Conference on Intelligent Robots and Systems,* pp. 680-687, 2016.

[29] E. Spyrakos-Papastavridis, P. R. N. Childs, J. S. Dai, "Passivity Preservation for Variable Impedance Control of Compliant Robots," *IEEE/ASME Transactions on Mechatronics,* doi: 10.1109/TMECH.2019.2961478.

[30] E. Spyrakos-Papastavridis, J. S. Dai, "Minimally Model-based Trajectory Tracking and Variable Impedance Control of Flexible-Joint Robots," *IEEE Transactions on Industrial Electronics,* doi: 10.1109/TIE.2020.2994886.

[31] S. Traversaro, D. Pucci, F. Nori, "A unified view of the equations of motion used for control design of humanoid robots," *On line, 2017. [Online]. Available: https://traversaro.github.io/preprints/changebase.pdf.*

[32] P. J. From et al., "On the Boundedness Property of the Inertia Matrix and Skew-Symmetric Property of the Coriolis Matrix for Vehicle-Manipulator Systems," *Journal of Dynamic Systems, Measurement and Control,* vol. 134, no. 4, 2012.

[33] A. van der Schaft, L_2-Gain and Passivity Theorem Techniques in Nonlinear Control, *Springer-Verlag, no. 2, 2000.*

[34] I. Barkana, "Defending the beauty of the invariance principle," *International Journal of Control,* vol. 87, no. 1, pp. 186–206, 2004.

[35] A. M. Giordano et al., "Dynamics and control of a free-floating space robot in presence of nonzero linear and angular momenta," *IEEE Conference on Decision and Control,* pp. 7527-7534, 2016.

[36] M. Mosadeghzad et al., "Optimal Human-Inspired Ankle Stiffness Regulation for Humanoid Balancing Control," *IEEE-RAS International Conference on Humanoid Robots,* pp. 902-907, 2014.

[37] E. Spyrakos-Papastavridis et al., "Online impedance regulation techniques for compliant humanoid balancing," *Robotics and Autonomous Systems,* vol. 104, pp. 85-98, 2018.

[38] E. Spyrakos-Papastavridis, P. R. N. Childs, N. G. Tsagarakis, "Variable impedance walking using time-varying Lyapunov stability margins," *IEEE-RAS International Conference on Humanoid Robots*, pp. 318-323, 2017.

[39] E. Spyrakos-Papastavridis et al., "Optically-regulated impedance-based balancing for humanoid robots," *IEEE-RAS International Conference on Humanoid Robots,* pp. 41-46, 2015.

[40] http://www.daran.tech/index.php?lang=en